Synthesis of Nanocrystalline $Gd_2Ti_2O_7$ by Combustion Process and its Structural, Optical and Dielectric Properties

Jeyasingh T[1], Saji S K[1] and P R S Wariar[1,a)]

[1]*Department of Physics, University College, Thiruvananthapuram-695034, Kerala, India*.

[a)] Corresponding author: prswariar1953@gmail.com

Abstract. Nanosized pyrochlore material Gadolinium Titanate ($Gd_2Ti_2O_7$) powder was prepared by modified single step auto-ignition combustion process. The phase formation has been investigated using X-Ray diffraction analysis (XRD). The crystalline pyrochlore phase is further confirmed by the presence of metal-oxygen bonds in the FT-IR spectra. XRD analysis revealed that $Gd_2Ti_2O_7$ has a cubic structure with Fd3m space group. The combustion powder was sintered to high density (97% of theoretical density) at ~1300^0 C for 4h and the surface morphology was examined by Scanning Electron Microscopy (SEM). The optical band gap of $Gd_2Ti_2O_7$ determined from the absorption spectrum is found to be 4.2 eV, which corresponds to direct allowed transitions. The dielectric measurements were carried out using LCR meter in the radio frequency region at room temperature. The sintered $Gd_2Ti_2O_7$ has a dielectric constant (ε_r) = 40 and dielectric loss (tan δ) = 0.01 at 1MHz.

Key words: combustion, dielectric properties, pyrochlore, sintered.

INTRODUCTION

Titanate pyrochlore, $A_2Ti_2O_7$, materials are important for their potential use as solid electrolytes and mixed ionic/electronic conducting electrodes [1], catalysts and ferroelectric/dielectric device compounds [2]. Compounds with the general formula $A_2B_2O_7$, exhibited interesting properties for application such as host matrices for nuclear wastes, high temperature pigments, thermal barrier coatings, oxygen sensors etc [3]. Pyrochlore structured materials are used in a variety of applications, such as anion and mixed conduction, Solid Oxide Fuel Cell (SOFC) electrolyte, magneto-resistance, dielectrics and electrocatalysts [4]. Some of the pyrochlores show good catalytic activity, high melting point, low thermal conductivity, high thermal and phase stability, which make them promising for the catalytic combustion applications and thermal barrier coatings [5,6].

Mostly "A" cation can be a trivalent rare-earth ion, but can also be a mono, divalent alkali ions, and "B" cation may be transition element or a post- transition metal give rise to the composition $A_2B_2O_7$ [7]. In pyrochlore structure, the larger "A" cation occupy the 16c sites and smaller "B" cation occupy 16d sites. Oxygen ions are located at the 48f, 8a and 8b positions. The stability of $A_2B_2O_7$ type pyrochlore structure is governed by the ratio of the ionic radii (r_A/r_B) of A and B cations, which extends from 1.46 to 1.78 [8]. Rare-earth pyrochlore ($Gd_2Ti_2O_7$) has been synthesized by different methods such as sol-gel [9], solid state reaction [10], chemical-coprecipitation, calcinations method [11] and pechini process. However, these methods involve multi-step complicated reaction routes with longer duration for synthesis and higher calcination temperature. To overcome all these disadvantages, we have made an attempt through a modified combustion technique to synthesize high phase pure Gadolinium Titanate ($Gd_2Ti_2O_7$) compound.

MATERIALS AND METHODS

Gadolinium oxide Gd_2O_3 (99.99% Purity, Sigma Aldrich) and Titanium dioxide TiO_2 (99.99% Purity, Sigma Aldrich) were used as the starting materials for the synthesis. Gd_2O_3 and TiO_2 were dissolved in nitric acid and mixed with distilled water to form an aqueous solution. Suitable amount of citric acid was added into the solution containing Gd^{3+} and Ti^{4+} metal ions, keeping the citric acid to cation ratio unity. The product was stirred well for uniform mixing, and then nitric acid and ammonium hydroxide were added to the system to adjust the oxidant fuel ratio. The solution containing the complex precursor at neutral pH (~7) was heated to about 250^0 C on a hot plate. The solution boiled on heating, which undergoes dehydration followed by decomposition leading to a smooth deflation producing a dark form. The form gets auto-ignited on persistent heating giving voluminous and fluffy combustion powder.

The as prepared powders were calcinated at 600^0C to remove the carbonaceous residues. XRD analysis was carried out using an X-ray powder diffractometer (Bruker AXS D8 Advance) with CuKα radiation (1.5406 Å). FT-IR spectra has been recorded with a Thermo-Nicolet Avatar 370, in the range 400–4000 cm^{-1}. The high resolution TEM images were taken on a Transmission Electron Microscope, Jeol-JEM 2100. The powders have been mixed with PVA and pressed to form cylindrical compacts at a pressure about 350 MPa using a hydraulic press, which then sintered at 1300^0C for 4 hrs. The SEM microstructure was obtained from Scanning Electron Microscope (JOEL, JSM-6390LV). The optical properties of $Gd_2Ti_2O_7$ nanopowder were measured using UV-Vis (Varian, Cary 5000) spectrophotometer in the range from 200-2000 nm. The dielectric studies were performed with LCR meter in the frequency range 50Hz to 5MHz.

RESULTS AND DISCUSSION

XRD ANALYSIS

Fig. 1 shows the X-ray diffraction pattern of the prepared combustion powder. The main diffraction peaks observed correspond to (222), (440) and (622) planes with the $2\theta \sim 30.36^0$ (100% relative intensity), 50.65^0 (60%) and 60.22^0 (50%) are confirming the presence of the ($Gd_2Ti_2O_7$) compound. The lattice constant has been determined from XRD data and found to be a = 10.1756 Å. The calculated lattice constant value is in good agreement with the standard JCPDS data (02-4207). The average crystalline size was calculated by using the Debye-Scherrer formula and found to be ~28 nm. From the XRD pattern no diffraction peak that could be related to impurity or secondary phase was observed.

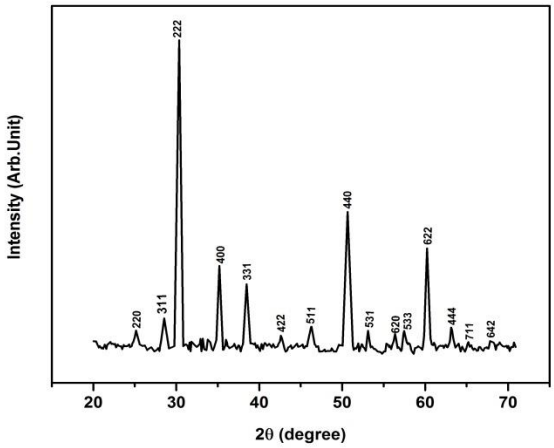

FIGURE 1. XRD pattern of $Gd_2Ti_2O_7$ powder

FT-IR SPECTROSCOPY

The FT-IR spectrum of the combustion product is shown in Fig. 2. FT-IR bands have been analyzed for further confirm the phase formation and identifying the functional group present in the compound. Weak absorption peaks in the region from $500\ cm^{-1}$ to $900\ cm^{-1}$ are assigned to Ti-O-Ti bending vibrations. The bands appearing between 1390-1500 cm^{-1} attributed the symmetric stretching mode of carbonyl functional group, which can be related to organic matter, probably originated from the incomplete decomposition of precursor at low calcination temperature (600^0C). There was a slight absorption of mode of CO_3^{2-} ion, though there were no additional peaks observed in the corresponding XRD spectrum. The band at 3421.7 cm^{-1} indicates the hydroxyl group (O-H) due to the presence of water observed from moisture. The formation of pyrochlore phase is further confirmed by the occurrence of metal-oxygen bond in the FT-IR spectra

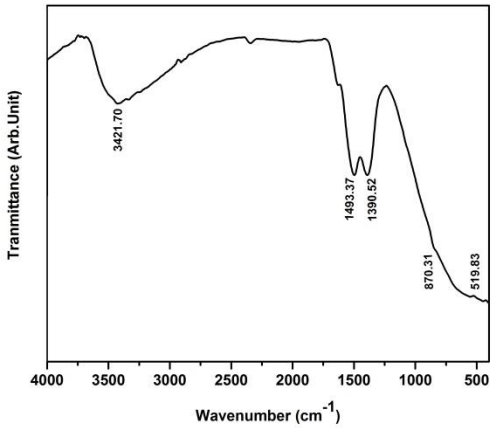

FIGURE 2. FT-IR spectrum of $Gd_2Ti_2O_7$ sample

TEM ANALYSIS

The TEM analysis can yield information such as particle size, size distribution and microstructure of the nanoparticles. The High Resolution Transmission Electron Micrograph (HRTEM) of $Gd_2Ti_2O_7$ nanopowder and selected area diffraction (SAED) pattern are shown in Fig. 3 (a,b). The high resolution TEM image revealed that nanoparticles had good crystalline structure and average particle size is 30 nm. The ring diffraction pattern is an indicative of the polycrystalline nature of the crystallites.

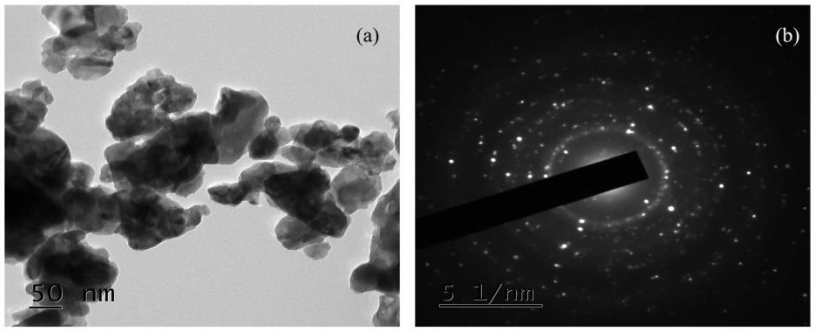

FIGURE 3. (a) HRTEM micrograph; (b) SAED pattern of $Gd_2Ti_2O_7$

UV-VIS-NIR ANALYSIS

The UV-Vis spectroscopy analysis is used to determine the optical band gap of the material with the help of absorption spectrum. Fig. 4(a) shows the UV-Vis-NIR reflectance spectrum of $Gd_2Ti_2O_7$ nanoparticles. According to Kubelka-Munk theory, the absorption coefficient of the material is given by $\alpha h\upsilon \approx B(h\upsilon - E_g)^n$, where B- constant, α – absorption coefficient, $h\upsilon$ – photon energy and Eg- bandgap. n=1/2 for a direct allowed transition (plotted as $(\alpha h\upsilon)^2$ versus $h\upsilon$) shown in Fig. 4(b). The extrapolation of straight line to $(\alpha hv)^2 = 0$ axis gives value of the optical band gap of the material, which is found to be 4.2 eV. $Gd_2Ti_2O_7$ nanopowder may be used as solar reflective as well as color pigment due to its high NIR reflectivity.

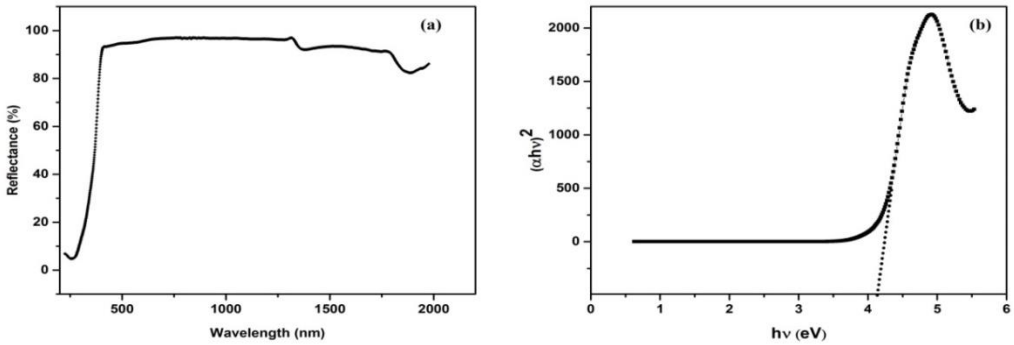

FIGURE 4. (a) UV-Vis reflectance spectrum of $Gd_2Ti_2O_7$; (b) optical band gap of $Gd_2Ti_2O_7$ sample

SEM ANALYSIS

The morphological features of the sintered pellet were obtained from High Resolution Scanning Electron Microscopy (HRSEM). Fig. 5 shows the SEM micrograph of $Gd_2Ti_2O_7$ samples showing well crystallized sub-micron grains with sharp grain boundaries and the grains are in different size varying from few nanometers to micrometer scales. No cracks were observed on the surface and the porosity was very less. The average grain size was determined from SEM micrograph to be around ~ 700 nm.

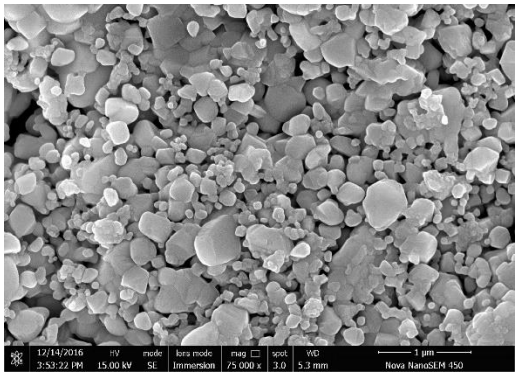

FIGURE 5. SEM image of sintered pellet of $Gd_2Ti_2O_7$

DIELECTRIC PROPERTIES OF $Gd_2Ti_2O_7$

The relative dielectric constant (ε_r) and loss factor (tan δ) of $Gd_2Ti_2O_7$ samples were studied from capacitance measurements by sandwiching the sintered specimen between two silver electrodes. The variation of frequency dependence dielectric constant and loss tangent are shown in Fig. 6. Generally, both dielectric constant and loss factor follow a power law dependence on frequency as ω^{n-1} ($n < 1$), where ω is the frequency, regardless of their physical and chemical natures [12]. The dielectric constant and loss factor decrease with the increase in frequency and dielectric constant (ε_r) = 40 and dielectric loss (tan δ) = 0.01 (1MHz) at room temperature.

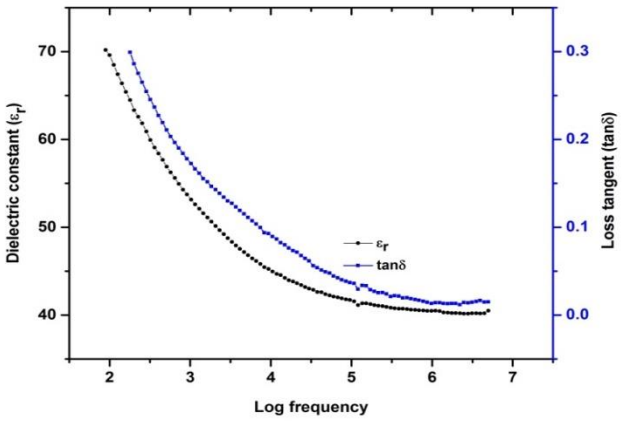

FIGURE 6. Variation of dielectric constant (ε_r) and loss tangent (tan δ) with frequency of $Gd_2Ti_2O_7$

The decrease in the dielectric constant with increasing frequency is attributed to Maxwell-Wagner interfacial polarization [13]. It is due to the fact that polarization does not occur instantaneously with the application of the electric field because of inertia and all the polarizations contribute, at low frequencies. When frequency increases, the dielectric constant decreases due to the large relaxation time [14]. The decrease of loss tangent (tan δ) with the increase of frequency may be on the basis of Koops phenomenological model [15]. The lower dielectric loss of the material is beneficial to fabricate low-loss microwave electronic circuits.

CONCLUSION

Nanocrystalline $Gd_2Ti_2O_7$ has been synthesized using modified combustion method. XRD analysis revealed that $Gd_2Ti_2O_7$ phase formation. The pyrochlore phase is further confirmed by the existence of metal-oxygen bonds in the FT-IR spectra. $Gd_2Ti_2O_7$ nanopowder may be used as solar reflective as well as color pigment due to its high NIR reflectivity (90-95%). The frequency dependence dielectric properties have been studied and lower dielectric loss of the material is beneficial to fabricate low-loss microwave electronic circuits.

REFERENCES

1. S.A. Kramer, H.L.Tuller, A novel titanate-based oxygen conductor $Gd_2Ti_2O_7$ Solid State Ionics 82 (1995) 15-23.
2. J.H. Lee, Y.M. Chiang, Pressure-induced pyrochlore-perovskite phase transformation in PLZST cermics, Journal of Electroceramics 6 (1) (2001) 7-12.
3. S.H. Oh, R. Black, E. Pomerantseva, J.-H. Lee, L.F. Nazer, Synthesis of a metallic mesoporous pyrochlore as a catalyst for lithium-O_2 batteries, Nat. Chem. 4 (2012) 1004-1010.

4. J. B. Goodenough, R.N. Castellano, J. Solid State Chem. 44 (1982) 108-112.
5. Y. Teraoka, K.-I. Torigoshi, H. Yamaguchi, T. Ikeda, S. Kagawa, J. Mol. Catal. A: Chem. 155 (1/2) (2000) 73.
6. H. Lehmann, D. Pitzer, G. Pracht, R. Vassen, D. Stover, J. Am. Ceram. Soc. 86(8) (2003) 1338.
7. A. Garbout, I. Ben Taazayet-Belgacem, M. Ferid, Structural, FT-IR, XRD and Raman scattering of new rare-earth-titanate pyrochlore-type oxides $LnEuTi_2O_7$ (Ln = Gd, Dy), Journal of Alloys and Compounds, 573 (2013) 43-52.
8. Ewing RC, Weber WJ, Lian J. J Appl Phys 2004;95:5949.
9. M.L. Pang, J. Fu, Z.Y. Cheng, Luminescent properties of $Gd_2Ti_2O_7:Eu^{3+}$ phosphor films prepared by sol-gel process, Materials Research Bulletin 39 (2004) 1607-1614.
10. M. Maczka, J. Hanuza, K. Hermanowicz, A.F. Fuentes, K. Matsuhira, Z. Hiroi, Temperature-dependent Raman scattering studies of the geometrically frustrated pyrochlores $Dy_2Ti_2O_7$, $Gd_2Ti_2O_7$, and $Er_2Ti_2O_7$, Journal of Raman Spectroscopy 39 (2008) 537-544.
11. Z.G. Liu, J.H. Ouyang, K.N. Sun, Electrical conductivity improvement of $Nd_2Ce_2O_7$ ceramic co-doped with Gd_2O_3 and ZrO_2, Fuel cells 11(2) (2011) 153-157.
12. Jonscher AK. Physical basis of dielectric loss. Nature 1975;253:717-719.
13. J.C. Maxwell, ATreatise on Electricity and Magnetism, vol. 2, Oxford University Press, Oxford, U.K, 1954 Section 328.
14. A.T. Raghavendar, K.M. Jadhav, Dielectric properties of Al-substituted Co ferrite nanoparticles, Bulletin of Materials Science 32 (2009) 575-578.
15. C.G. Koops, On the dispersion of resistivity and dielectric constant of some semiconductors at audiofrequencies, Physical Review 83 (1951) 121-124.